

# THE EFFECT OF DELAMINATION GEOMETRY ON THE BUCKLING AND FAILURE OF GFRP PLATES

G.J. Short, F.J. Guild and M.J. Pavier

*Department of Mechanical Engineering, University of Bristol  
University Walk, Bristol, BS8 1TR, U.K.*

**SUMMARY:** Delaminations in composite laminates can cause a reduction in compressive strength due to buckling of the delaminated plies. The aim of this work is to study the effect of delamination geometry on the compressive behaviour of layered composites using finite element models and closed form solutions with isotropic properties to identify trends in behaviour. These studies were then related to experimental observations in glass fibre reinforced plastic test specimens. Three distinct modes of panel behaviour (delamination buckling, global plate buckling and mixed mode buckling), dependant on delamination geometry, were identified from this isotropic modelling. These trends were correlated with experimental data, which showed this technique to be valid for predicting buckling behaviour in layered composite materials.

**KEYWORDS:** Delamination, Buckling, Finite Element Analysis, Failure, Laminates

## INTRODUCTION

Structures of layered composite materials offer many advantages in terms of manufacturing flexibility and the ability to easily tailor the components material properties to its task. In addition to the usual imperfections associated with metallic structures, laminated composites are susceptible to a range of other defects such as ply breakage, matrix cracking and delamination. Delaminations (areas of disbonding between adjacent plies) may form as a result of imperfections during component production, or from sources such as impact damage whilst in-service.

From whatever source, previous work [1] has shown the mechanism of compressive strength reduction typically results from the plies above the delamination buckling out of plane. Once this buckling occurs, the remaining plies become subject to bending in addition to the in-plane compressive load. The stresses in the remaining plies are therefore higher than would exist in an undelaminated panel leading to a reduced failure load.

The aim of the present work is to study the effect of delamination using a model with isotropic material properties to clarify the effects of changes in the delamination geometry. This approach allowed trends for sub-laminate (groups of plies above and below the delamination)

response and its effect on failure load to be identified using simple analytical modelling that would not be appropriate for layered composite materials due to the in-plane material orthotropy. Finite element analysis of a range of delaminated isotropic models was also carried out to verify the results, and the general trends were compared to experimental results carried out on glass fibre reinforced plastic (GFRP) panels containing artificially introduced delaminations.

### ISOTROPIC MODELLING

Finite element analysis was used to predict the buckling and post-buckling response of a delaminated isotropic panel, for different delamination sizes and depths. As the plate was flat, results for delamination depth would be symmetric either side of the mid plane. For comparison between isotropic model and experimental results, the delamination size and depth were normalised against the dimensions of the plate, though for the purposes of the analytical modelling, the plate had to be sufficiently slender to allow the panel to be assumed to be thin. Figure 1 shows the range of geometry studied.

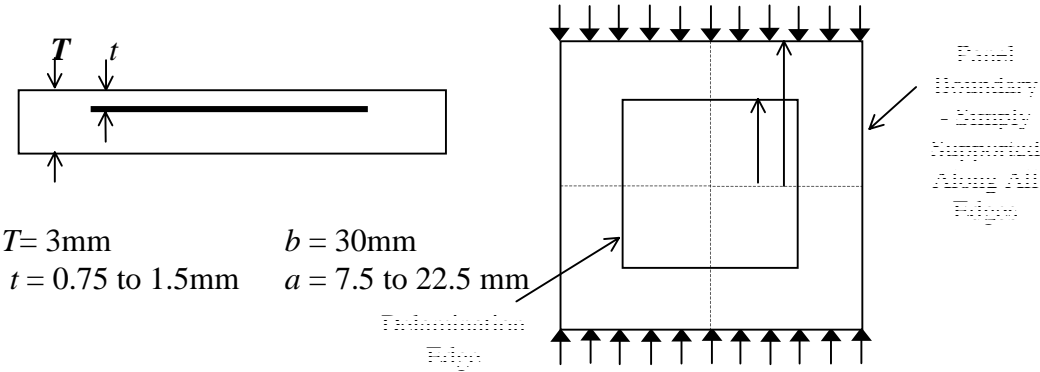


Figure 1 : Diagram of delamination geometry

The finite element mesh is shown in Figure 2. A layer of 20 node isotropic brick elements of thickness  $t$  was used for the material above the delamination while another layer of thickness  $T-t$  was used to model the remaining thickness of material. The area of the mesh immediately above the delamination was given an initial out of plane displacement at its centre to initiate buckling. All edges of the model were constrained using simply supported conditions and compressive pressure loading applied to two parallel edges of the model. A non-linear large displacement analysis was carried out, with Patran v7.5 used for pre-processing and ABAQUS v7.5 used for analysis and post-processing, running on a Silicon Graphics Origin 200 workstation.

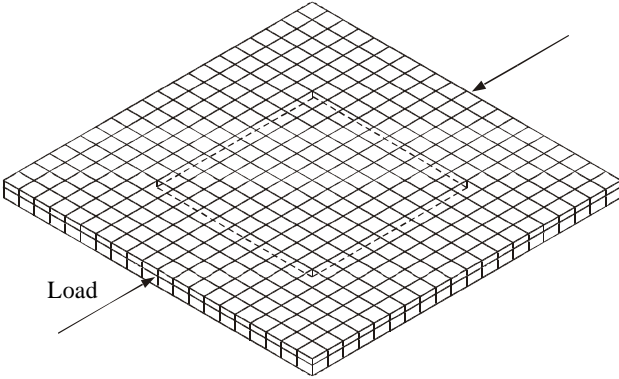


Figure 2 : Finite element model of delaminated panel

Nine models were analysed to investigate the primary buckling. From these results three distinct buckling modes were identified. Table 1 outlines the delamination geometry as well as model name and initial sub-laminate response, determined by measuring the out of plane deflection at the centre of the top and bottom surfaces. It can be seen that the models containing small delaminations near the centre line of the panel produce a global plate buckling response, characterised by both sub-laminates deflecting in the same direction with the same magnitude. A typical deflection plot of the nodes at the centre of the sub-laminates, for this case, is shown in Figure 3.

Another mode of behaviour was identified for large delaminations close to the surface of the model. Such delamination buckling was characterised by initial buckling of the upper sub-laminate resulting in downward deflection of the lower sub-laminate, due to unsymmetric loading, as shown in Figure 4.

Thirdly, an intermediate, or mixed mode, response was observed in model 075LD05 which was characterised by the upper and lower sub-laminate deflecting in the same direction, but not with the same magnitude.

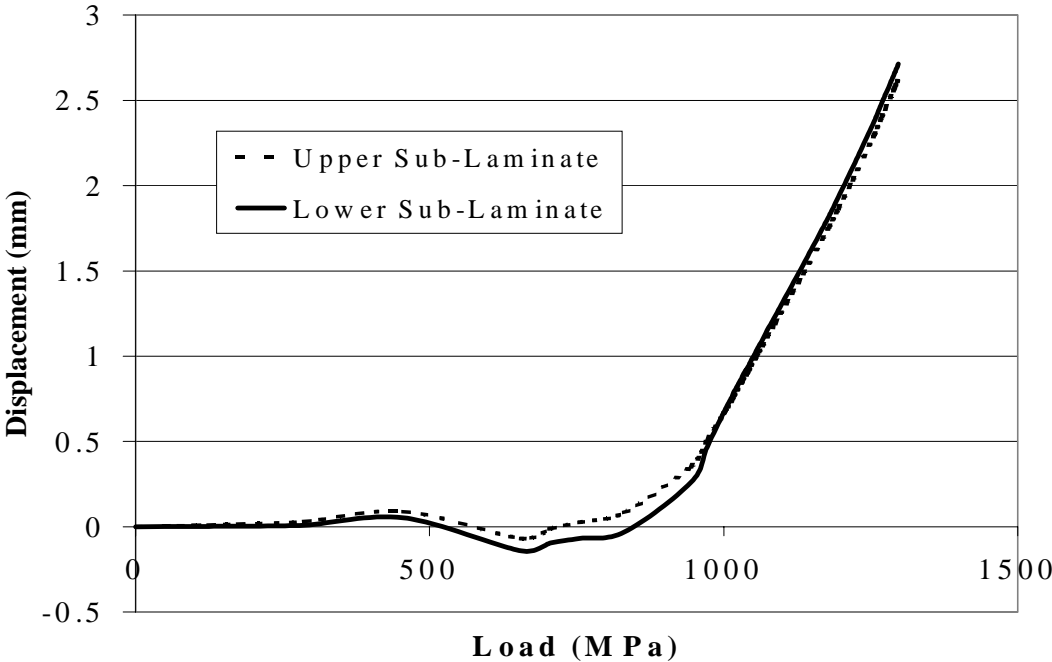


Figure 3 : Out of plane deflection versus applied load for global buckling

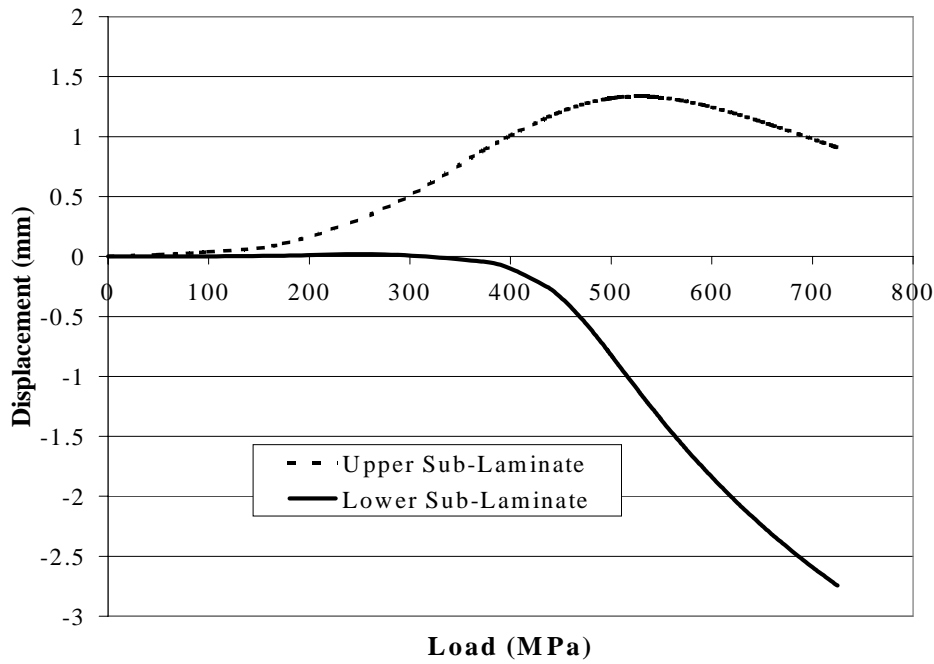


Figure 4 : Out of plane deflection versus applied load for delamination buckling

Table 1 : Initial response of delaminated models to compressive load

Model Name	t (mm)	T (mm)	t/T	a (mm)	b (mm)	a/b	Initial Response
075LD025	0.75	3.00	0.25	7.5	30	0.25	Delamination
075LD05	0.75	3.00	0.25	15	30	0.5	Mixed Mode
075LD075	0.75	3.00	0.25	22.5	30	0.75	Delamination
100LD025	1.00	3.00	0.33	7.5	30	0.25	Global
100LD05	1.00	3.00	0.33	15	30	0.5	Global
100LD075	1.00	3.00	0.33	22.5	30	0.75	Delamination
150LD025	1.50	3.00	0.5	7.5	30	0.25	Global
150LD05	1.50	3.00	0.5	15	30	0.5	Global
150LD075	1.50	3.00	0.5	22.5	30	0.75	Global

Analytical modelling was also carried out in an attempt to predict the modes of sub-laminate behaviour, using the FEA results as validation. It was hoped that this approach would allow the behaviour of delaminated panels with any delamination geometry to be predicted easily.

The method used was to consider the area of upper sub-laminate above the delamination, and the lower sub-laminate, as two separate plates, and evaluate the buckling load for each plate separately (see Figure 5). This was done using Eqn 1 to calculate the critical load, where  $E$  is the modulus of elasticity,  $\nu$  is Poissons ratio,  $t$  is the thickness of the panel and  $b$  is the panel width [2]. The factor  $K$  varies according to panel aspect ratio and edge conditions. Whichever had the lower critical load was then judged to have buckled first. A buckling mode map was then created by plotting a theoretical line of transition between delamination and global buckling on a graph of  $t/T$  versus  $a/b$  at which the critical loads for the two sections of the model were equal.

$$\sigma_{cr} = K \frac{E}{(1-\nu^2)} \left( \frac{t}{b} \right)^2 \quad (1)$$

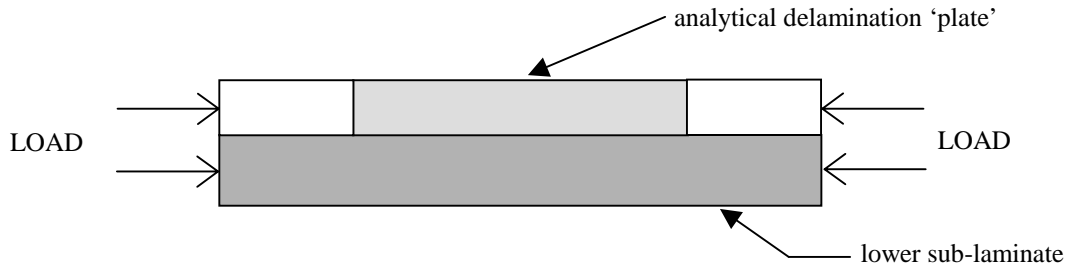


Figure 5 : Diagram of plate areas used for analytical method

To match the finite element models, the boundary conditions for the lower sub-laminate were simply supported along all edges, but the support conditions around the edge of the delamination will vary as its area increases. When the delamination area is small the edge conditions will be built in along all edges, due to the constraint of the rest of the upper sub-laminate. However, as the delamination area increases to its limit where  $a/b=1$ , the edge conditions will tend to simply supported. For this reason, the calculations were carried out for each boundary condition. For a panel with an aspect ratio equal to 1,  $K=3.29$  for simply supported conditions, and  $K=7.7$  for all edges built in.

Using these results a graph of  $a/b$  versus  $t/T$  was generated and the two transition lines plotted onto it. The resulting buckling mode map, with the finite element model geometries overlaid for comparison, can be seen in Figure 6. The lower central area represents the geometries for which global buckling occurs, with the areas the other side of the transition line representing areas of delamination buckling. Agreement between the results for the FEA (Table 1) and analytical models in the global region is generally very good.

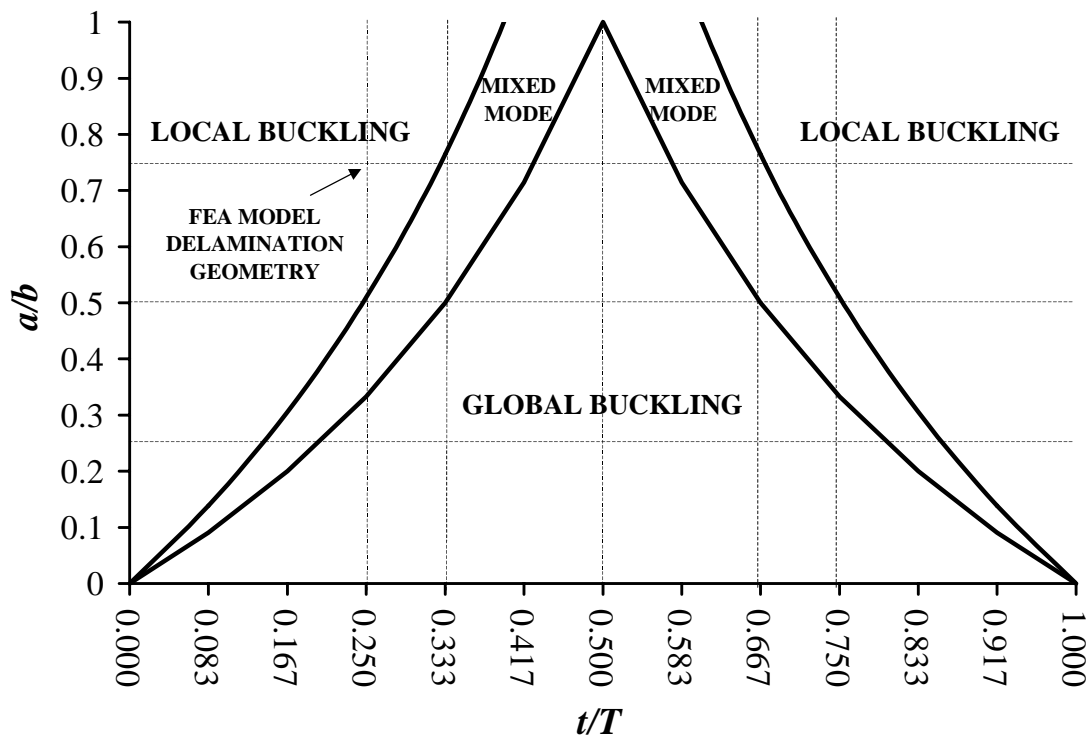


Figure 6 - Buckling mode map from isotropic model results

## EXPERIMENTAL WORK

Compression tests were carried out on specimens containing artificially implanted delaminations to compare trends in delaminated composite panels with those predicted by isotropic modelling. An anti-buckling guide (ABG) was used to prevent gross buckling of the specimens and the out of plane deflection on both faces of the specimen at the centre of the delamination area were recorded during the test using two calibrated LVDT's.

Specimens were manufactured by hand lay-up, and cured using the vacuum bag method, from I.C.I. Fiberite unidirectional glass fibre/epoxy pre-preg with material properties of  $E_{11} = 46.0$  GPa,  $E_{22} = E_{33} = 13.0$  GPa,  $G_{23} = 4.6$  GPa,  $G_{13} = G_{12} = 5.0$  GPa,  $\nu_{23} = 0.42$  and  $\nu_{13} = \nu_{12} = 0.3$ . The lay-up used for all tests was  $[0,+45,-45,0]_s$  which produced specimens with an average thickness of 2.4mm. Artificially delaminated specimens were created by inserting 10 $\mu$ m thick squares of PTFE film of the required size and at the correct inter-ply position to prevent ply to ply bonding. In this work, three through-thickness positions were used: position A between the first and second, 0 and +45 plies, position C between the third and fourth, -45 and 0 plies and position D centrally between two 0 plies. The delamination geometries selected for this study are shown in Table 2.

For each delamination geometry three coupons were tested and to maintain consistency were cut from a single plate. For undamaged specimens overall dimensions of the plates were 165mm x 210mm and for specimens containing artificial damage, plates were manufactured to dimensions of 185mm x 210mm, to allow some adjustment during cutting to centre the damage within the coupon. Specimens of 200mm x 50mm were then dry cut from these plates using a diamond encrusted edge slitting saw.

Table 2 : Delamination geometries studied experimentally

No. Of Specimens	Delam. Size	Delam. Position
6	Undamaged	Undamaged
3	25 x 25	'A'
3	25 x 25	'C'
3	25 x 25	'D'
3	15 x 15	'A'
3	10 x 10	'A'

Compression testing was carried out on a Zwick 1478 test machine with failure load, as well as sub-laminate deflections from the LVDT's, being recorded. The failure loads of the flat test coupons are shown below in Table 3.

Table 3 : Experimental failure loads of delaminated test coupons

Specimen Geometry	Specimen No. (Failure Load kN)			Average	Initial Response
	1	2	3		
Undamaged	42.9	45.8	45.6	44.8	-
25mm 'A'	36.6	37.8	38.6	37.7	Delamination
25mm 'C'	30.5	31.6	30.8	30.9	Mixed Mode
25mm 'D'	33.2	34.9	33.6	33.9	Global
15mm 'A'	38.8	41.1	40.9	40.3	Delamination
10mm 'A'	39.1	43.2	39.8	40.7	Delamination

This failure load data indicates that sub-laminate response, due to delamination geometry has a large effect on the compressive strength of the panels. This is best demonstrated with the tests on panels containing the 25mm square delaminations. With the delamination in the 'A' position, the coupon retained a high level of compressive strength, showing a 20% reduction compared to the undamaged panels. As has been reported previously [3] panel failure is governed by fibre failure of the zero degree plies in the laminate. In the 25'A' case the LVDT data (Figure 7) indicates that the surface (zero) ply buckles first and contributes little stiffness to the rest of the panel beyond this point. In this case, the upper sub-laminate is sufficiently slender that, once buckled, the distribution of load in the rest of the panel is not significantly disturbed.

For the 25'C' specimens the strength reduction was much greater - the failure load was reduced by 33% compared to the undamaged specimen. The LVDT output for the 25'C' specimens (Figure 8) shows a level of mixed mode sub-laminate response, with both sub laminates deflecting the same direction, but with significantly different magnitudes of displacement. The increased bending stresses in the lower sub-laminate accounts for the reduced failure load compared to the 'A' specimen.

The 25'D' specimen consistently showed greater compressive strength compared to the 25'C' specimens, indicating that a global response produces less bending stresses compared to mixed mode response. As was expected, the compressive strength increased as the delamination size was reduced.

To assess whether the results from isotropic modelling were relevant to the experimental results the responses of the all the delamination geometries studied experimentally (shown in Table 3) were overlaid onto the buckling mode map, with encouraging agreement. This is shown in Figure 9.

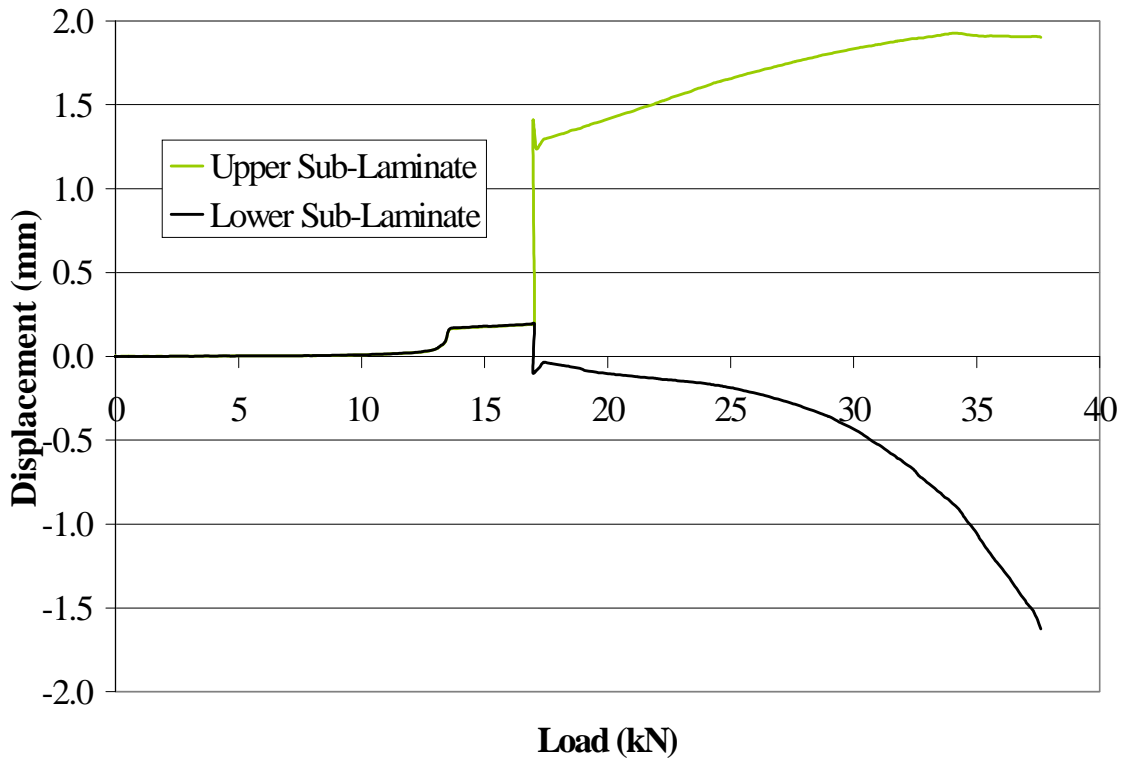


Figure 7 : LVDT sub-laminate displacement for specimen 25'A'

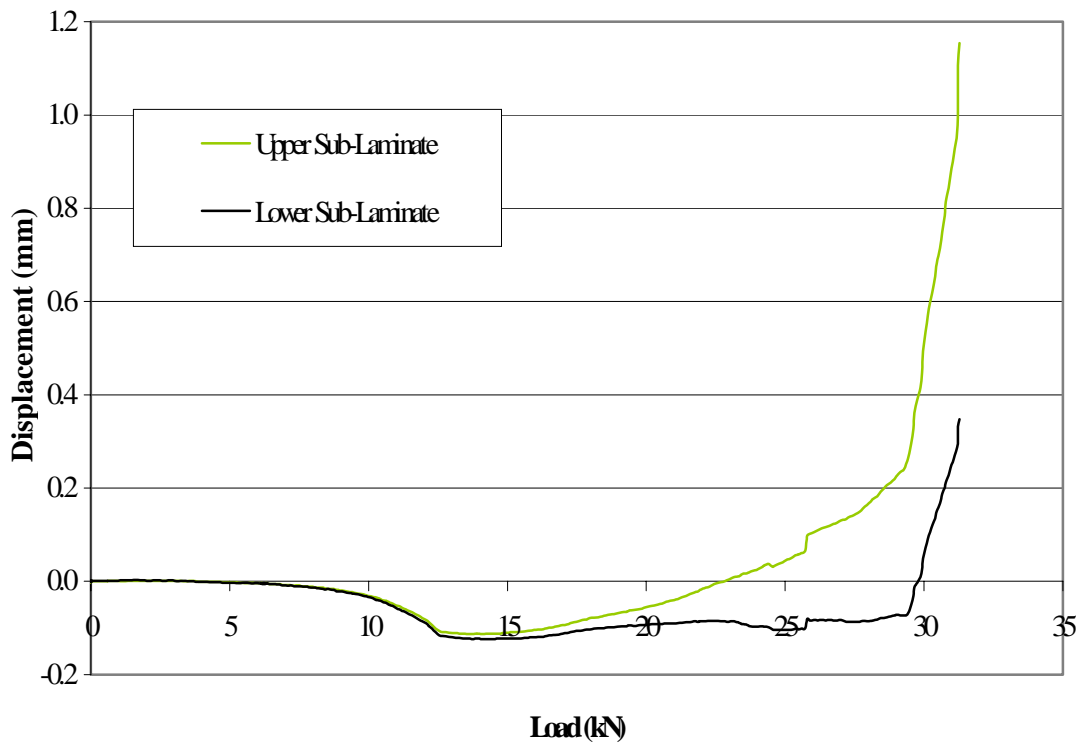


Figure 8 : LVDT sub-laminate displacement for specimen 25'C'

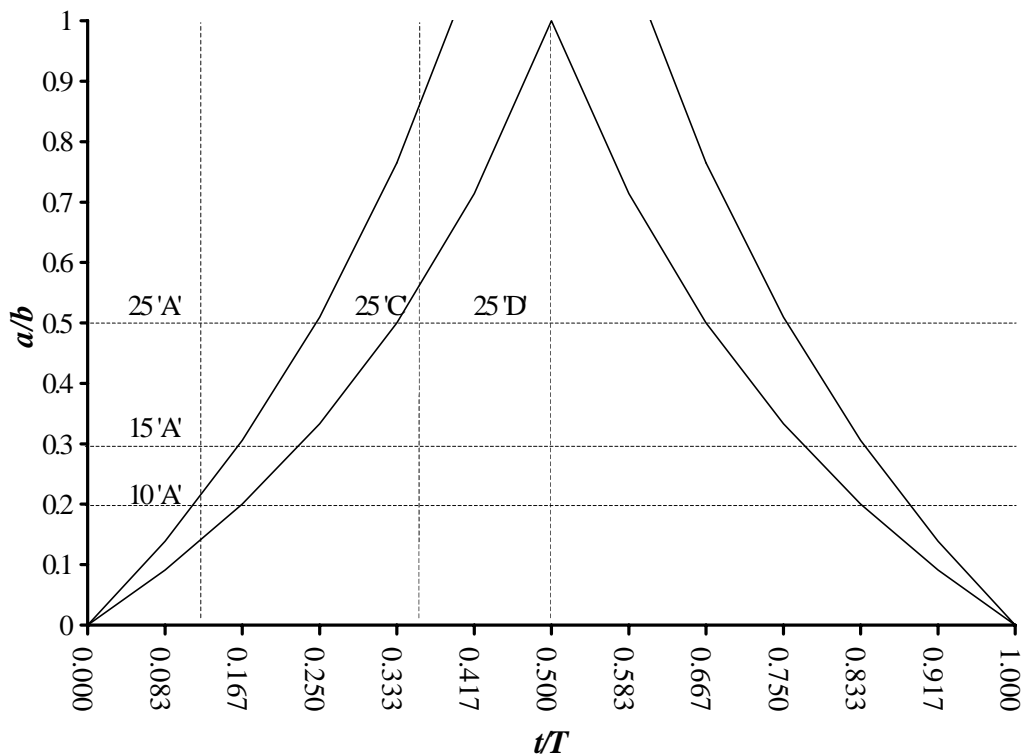


Figure 9 : Experimental results overlaid onto buckling mode map

## DISCUSSION

Comparison between the experimental results and isotropic models show encouraging agreement in terms of buckling mode prediction, with only minor disagreement at the limits of the delamination geometry studied.

The experimental results indicate that the 'C' position represents the worst-case for through the thickness delamination position, showing lower compressive strength compared to the 'A' and 'D' positions. For the 'A' position delaminations, where the lower sub-laminate is very much stiffer compared to the plies above the delamination, load is reasonably evenly transferred to the remaining plies after surface ply buckling. For the 'C' and 'D' positions the failure load was much less, as expected, with the mixed mode response of the 'C' position delamination being more critical than the global response induced by the geometry of the 'D' position delamination.

Initial buckling of a delamination highly influences the panel's residual compressive strength and it has been shown that specimen failure is linked to the compressive failure of the zero degree plies, which carry the majority of the compressive load in the specimen. If a zero degree ply fails in a critical area of the panel (the sub-laminate containing the most zero plies), failure is initiated due to the sudden loss of load carrying capacity and the transfer of load to the remaining plies in the laminate. In a post-buckled delaminated panel the compressive stresses are a combination of in-plane loading and bending induced compressive stresses on the inner surface of the buckle; hence failure of individual plies, and consequently the panel, is influenced by the magnitude of sub-laminate deflection.

## **CONCLUSIONS**

Analysis of delaminated panels with isotropic material properties shows that delamination geometry influences compressive strength. When a delamination is large and close to the surface a delamination buckling mode occurs causing a small reduction in compressive strength. If the delamination has a small area and is deep within the panel, a global buckling mode occurs, with again a small strength reduction. Between these two extremes a mixed mode occurs, causing an increased strength reduction.

Tests on delaminated GFRP specimens show that these isotropic analyses indicate trends which can be observed in experiments on orthotropic materials.

## **ACKNOWLEDGEMENTS**

Mr G J Short is supported by an EPSRC Studentship Award No. 97700381.

## **REFERENCES**

1. Pavier, M.J. and Clarke, M.P., "Finite element prediction of post impact compressive strength in carbon fibre composites", *Composite Structures*, Vol. 36, 1996, pp. 141-153.
2. Roark, R. J., *Roark's Formulas For Stress And Strain*, McGraw-Hill Book Co., 1965.
3. Clarke, M.P., "The effect of low velocity impact damage on the compressive properties of carbon fibre reinforced composites", PhD Thesis, University of Bristol, 1997.